3C-3D VSP: Normal moveout correction and VSPCDP transformation

Jitendra S. Gulati[*], Robert R. Stewart[*], Janusz Peron[+] and John M. Parkin[+].

* CREWES Project, + Western Atlas Logging Services.

ABSTRACT

In this paper, we address issues related to the normal moveout correction and VSPCDP transformation of 3C-3D VSP data. A proof is presented to show that in a horizontally layered isotropic earth the traveltime-distance (*t-x*) formulae for signals recorded in a VSP survey is hyperbolic. Synthetics corrected using amplitude semblance analysis show that events are corrected to normal incidence times with remarkable accuracy. Data from the Blackfoot 3C-3D VSP survey corrected to normal incidence time after amplitude semblance analysis show good correlation with that corrected using raytracing. A Dix formula is then used to estimate interval velocities below the total depth of the well from the stacking velocities obtained during the moveout correction.

The stacking velocities obtained during the moveout correction are used in an approximate VSPCDP transformation of the VSP data. Comparison of reflection points mapped using the approximate method with those using a raytracing method for synthetics show that the approximate method maps the reflections accurately for all practical purposes. The same approximate procedure applied to the Blackfoot 3C-3D VSP resulted in a 3-D image very similar to that obtained using a raytracing method.

These methods developed for a horizontally layered isotropic earth are an efficient way to obtain high-resolution 2-D/3-D seismic images in simple geologies. In complex geologies, however, they could precede more accurate imaging methods like migration to give a rough idea about the geology.

INTRODUCTION

The vertical seismic profile (VSP) is a technique that has primarily been used to identify and correlate major reflectors across log, VSP and surface seismic data (Hardage, 1983). Multi-receiver walkaway VSPs are used to obtain 2-D seismic images near the borehole. However, since our regions of interest are usually volumetric, there is a need for high-resolution 3-D images around the borehole. The 3-D VSP with an areal distribution of sources and several downhole receivers is one such technique that holds great promise in obtaining high-resolution images around the borehole. It was with this purpose that the first (to our knowledge) simultaneous land 3C-3D VSP and surface seismic survey was conducted over the Blackfoot field in Alberta, Canada. With frequent 3-D VSP acquisition likely in the near future, it is

essential to develop methods to process the 3-D VSP data. Most existing 2-D VSP processing methods can be used for processing the 3-D VSP data. However, methods like normal moveout correction, VSPCDP transformation (Wyatt and Wyatt, 1984) and migration which require a model cannot be directly used to process the 3-D VSP data. These either need to be adapted to the 3-D VSP survey or a different approach is required to obtain a 3-D seismic image near the borehole. In this paper, we address issues related to the normal moveout correction and VSPCDP transformation of 3-D VSP data and demonstrate the successful implementation of two new methods.

Conventionally, raytracing is used to correct the VSP data to normal incidence time. Well-logs and other velocity information from the area provide a starting velocity-depth model in the interactive moveout correction by raytracing. However, due to factors like velocity anisotropy, these starting estimates of the model which are based on vertical times in general do not agree with estimates from slant or far-offset times (Dillon and Thomson, 1984). Thus, the slant raypath arrivals from far-offsets force the moveout correction to be done with extreme accuracy (Kohler and Koenig, 1986). This makes it a time-consuming process in the 3D context where the data volume is large and model building comparatively difficult.

Other moveout correction methods such as in Moeckel (1986) and the parabolic approximation used in Zhang et. al. (1995) also require a velocity model. These methods calculate the root mean square (*rms*) velocity from a model to correct the VSP data to normal incidence time. However, from surface seismic surveys, we know that the stacking velocity is greater than the *rms* velocity (Al-Chalabi, 1973). Analogous to this, it would mean that the above approximation methods may not give the optimum stack result. In such cases, a statistical moveout correction method similar to the amplitude semblance analysis (Taner and Koehler, 1969) used in surface seismic surveys is desired. Byun et. al. (1988) use amplitude semblance analysis on VSP data in their study on anisotropic velocity analysis. However, the authors are not aware of a method in literature to correct VSP data to normal incidence time using semblance analysis. Also a power series expansion of the $t^2(x^2)$ curve for VSP surveys over a horizontally layered earth similar to the one for surface seismic surveys is unknown to the authors.

The VSPCDP transformation is a technique that transforms the VSP data from the depth-time domain to the more familiar surface seismic offset-time domain (Wyatt and Wyatt, 1984). Conventionally, VSPCDP transformation is performed using a 2-D raytracing routine to first map the reflected signals and then transform the reflected signals from the depth-time domain (VSP domain) to the offset-time domain. Similarly, 3-D raytracing can be used in mapping the reflected signals from a 3-D VSP survey. Although a raytracing approach is accurate in mapping the reflection points, approximate mapping methods such as in Stewart (1985) and Stewart (1991) would give high-resolution seismic images with reasonable accuracy in simple geologies. Also 3-D raytracing maybe a time-consuming process and likely to be unnecessary in simple geologies.

In this paper, we first show that the traveltime-distance (*t-x*) relationship for signals recorded in a borehole is hyperbolic in a two-term truncation of the power series expansion of the $t^2(x^2)$ relationship. The hyperbolic relationship then provides a

statistical framework to correct the 2-D/3-D VSP data to normal incidence time from the surface. Data from the Blackfoot 3C-3D VSP survey are successfully corrected to normal incidence time using the hyperbolic moveout formula. A Dix formula is also used to estimate interval velocities below the total depth of the well from the stacking velocities.

Next we assume a homogenous single-layered earth and use the stacking velocities to approximately map the reflection points in the VSPCDP transformation process. This method which can easily be used for any VSP acquisition geometry is used in the VSPCDP transformation of the Blackfoot 3C-3D VSP data to obtain 3-D images around the borehole. At the time of going to press, these methods were successfully tested on both P-P and P-S arrivals on a synthetic, however, they were applied only to the vertical component of the Blackfoot 3C-3D VSP experiment.

NORMAL MOVEOUT CORRECTION

For surface seismic surveys, Taner and Koehler (1969) used a power series expansion of the parametric traveltime-distance equations and showed that the traveltime-distance relationship for signals reflected in a horizontally layered earth is hyperbolic. This relation provides a statistical framework in the normal moveout (NMO) correction of surface recorded signals in the common midpoint (CMP) domain. In Appendix A, we present an equivalent series expansion for VSP recorded signals and show that the traveltime-distance formula is hyperbolic for VSP recorded signals as well. This relation presents us an opportunity to NMO-correct VSP recorded signals in a manner similar to that performed in surface seismic surveys.

VSP moveout correction method

Unlike surface recorded signals, the locus of reflection points for each source-receiver pair in VSP surveys changes with reflector depth. It tends towards the source-receiver midpoint with increasing depth in a horizontally layered earth (see Dillon and Thomson, 1984 for excellent examples). Therefore, the VSP data cannot be sorted in the CMP domain as in surface seismic surveys. Also, the *rms* velocity (Equation A6) for reflected signals in the VSP geometry changes with the receiver depths/locations. This implies that to use the inherent data redundancy, VSP data needs to be sorted in the receiver domain for implementation of a NMO correction method similar to the one used in surface seismic surveys. Figure 1 shows the difference between the sorting of surface seismic and VSP data.

Moveout correction of pure P-wave arrivals

After the vertical component data is sorted into the receiver domain, Equation (A10) is used on the first-break picks to get the zero-offset time of the direct arrivals (t_{0d}). Further, amplitude semblance analysis (see Taner and Koehler,1969 for details) of the reflected arrivals based on Equation (A7) gives the zero-offset time (t_{0r}) for each of the reflected arrivals in the sorted data. The quantities t_{0d} and t_{0r} are then added to obtain the normal incidence time of the reflected arrivals. Figure 2 shows the steps followed in correcting the reflected arrivals to normal incidence time.

SYNTHETIC

Synthetic P-wave traveltimes were generated for a model (Figure 3) using raytracing. The borehole receivers are placed at depths 500m and 1000m with source offsets for each receiver varying from 50m to 2450m. Figure 4 shows the traveltimes of the P-wave reflected arrivals for the model with borehole receiver at 500m depth; the first event representing the P-wave direct arrival. Following the steps outlined above, the normal incidence times (Figure 5) for each of the reflected events were determined. To simulate amplitude semblance analysis, a least-squares solution to the traveltimes was used to calculate the normal incidence times of the reflections. In Figure 5 we observe that the estimated times match remarkably well with the actual times, with errors for all events being less than 2ms. Similar results were observed for the borehole receiver at 1000m depth.

BLACKFOOT 3-D VSP

The Blackfoot 3-D VSP data was acquired by simultaneously recording the shots used for a surface 3-D survey. As the survey was designed for the 3-D surface acquisition, the acquired 3-D VSP data lacks regularity with the surface shots randomly scattered for different receiver depths (see Zhang et al., 1996 for survey details). Data from the vertical component of the 3C-3D VSP experiment was first corrected to normal incidence times using conventional 2-D raytracing routine and later using amplitude semblance analysis. As the geology of the area is known to be simple, data from all shot locations for each receiver were analyzed together in the semblance analysis. However, several criteria such as azimuth and source-receiver offset could be used to sort the data in the receiver domain before semblance analysis. As model building is unnecessary in moveout correction by semblance analysis, one can analyze the data separately based on the above criteria with relative ease.

Upgoing waves from borehole receivers at depths 400m and 910m are used to compare the results of the two moveout correction methods. Upgoing waves corrected to normal incidence times after semblance analysis correlate very well with that corrected using raytracing (Figures 6 and 7). It is observed that amplitude semblance analysis performs marginally better than raytracing on the data from receiver depth of 910m.
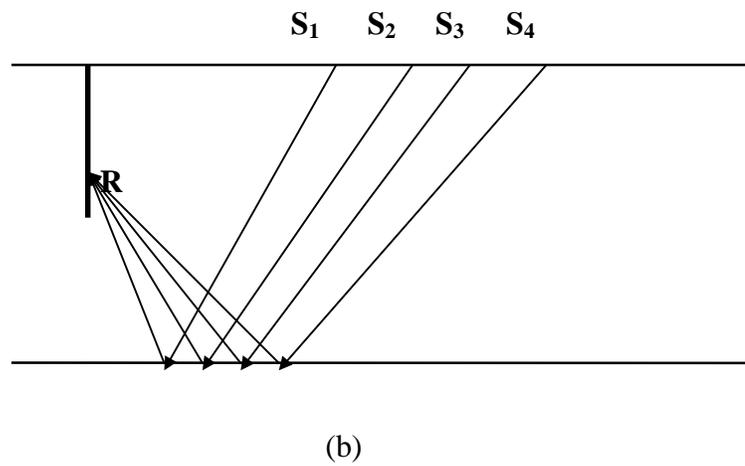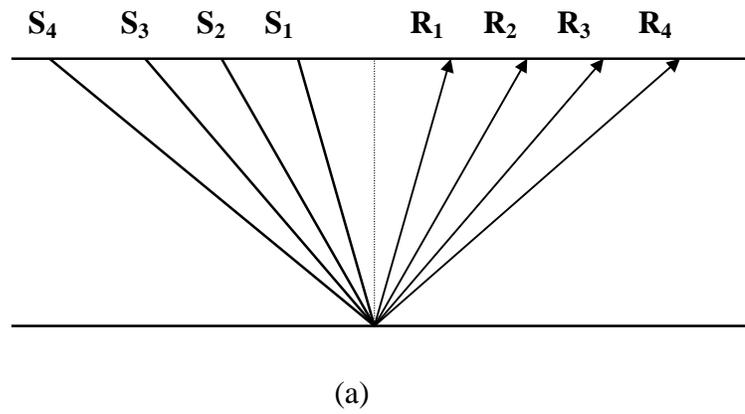
(a)

(b)

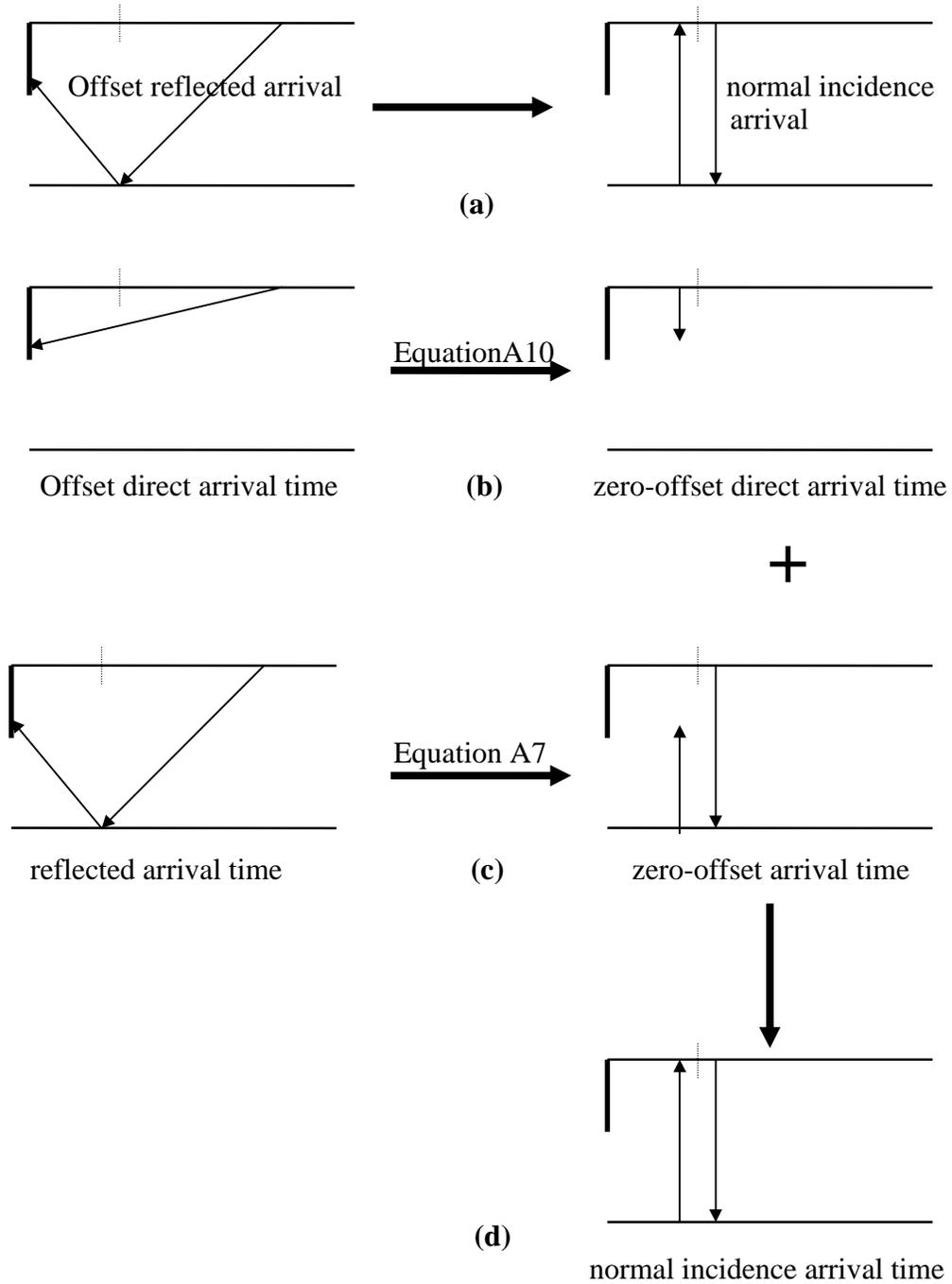Fig. 1. (a) Surface seismic data sorted in the CMP domain. (b) VSP data sorted in the receiver domain.

(a)

Offset reflected arrival → normal incidence arrival

(b)

Offset direct arrival time → EquationA10 → zero-offset direct arrival time

+

(c)

reflected arrival time → Equation A7 → zero-offset arrival time

(d)

normal incidence arrival time

Fig. 2.(a) The objective is to correct the arrival time of the reflected wave to a normal incidence time. (b) Correct the direct arrivals to a zero-offset time using Equation A10. (c)Correct the reflected wave arrival time at the receiver to zero-offset reflection time using Equation A7. (d)Adding the results of (b) and (c) then gives the normal incidence time for the reflected event.
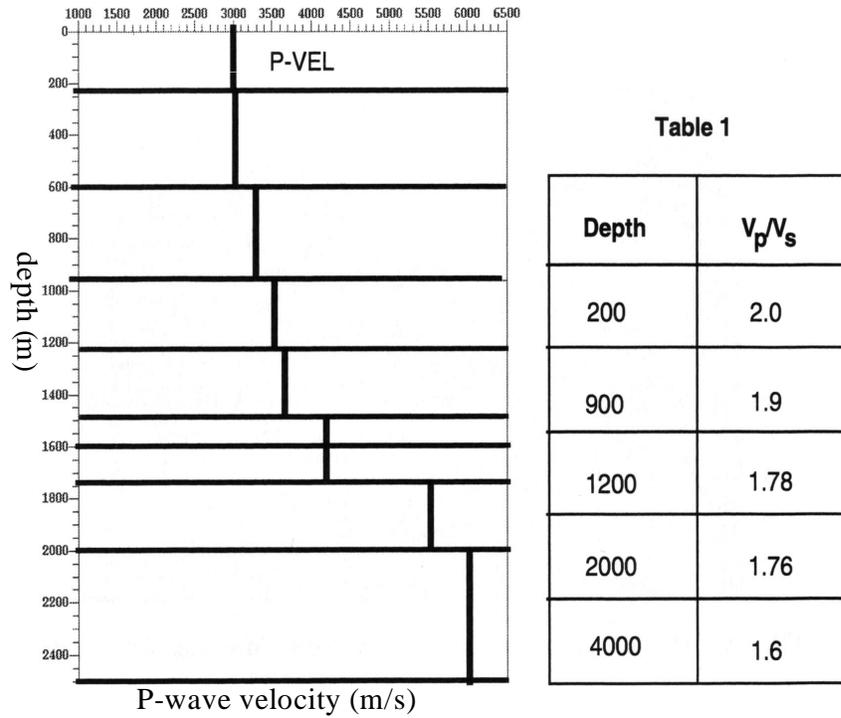
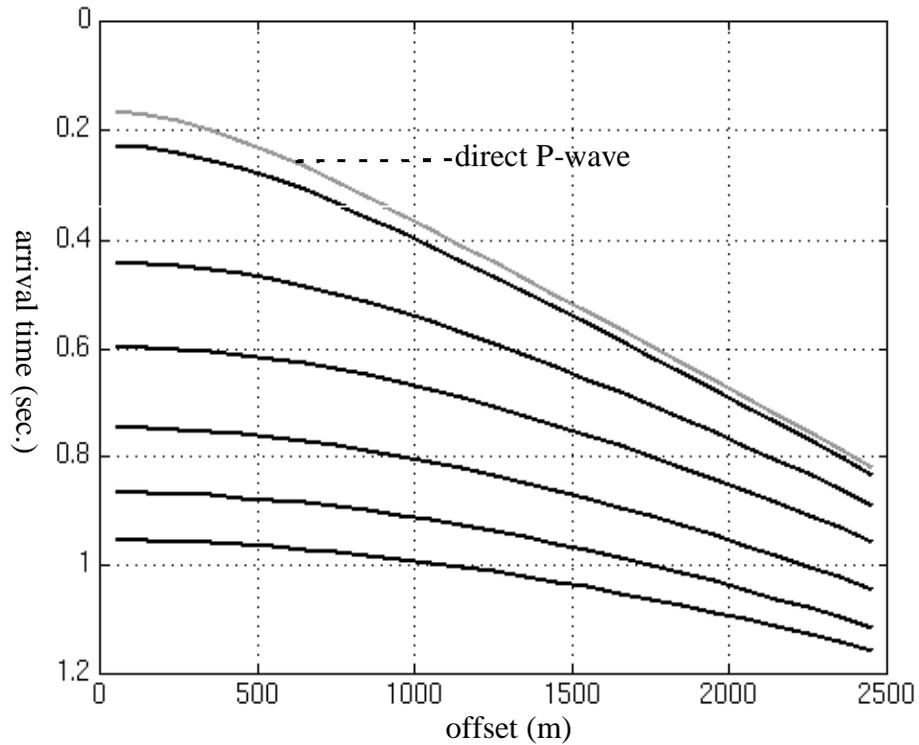Fig. 3.Elastic model used to generate P-P and P-S traveltimes for receiver in borehole (from Zhang et al., 1996)

Depth	V_p/V_s
200	2.0
900	1.9
1200	1.78
2000	1.76
4000	1.6

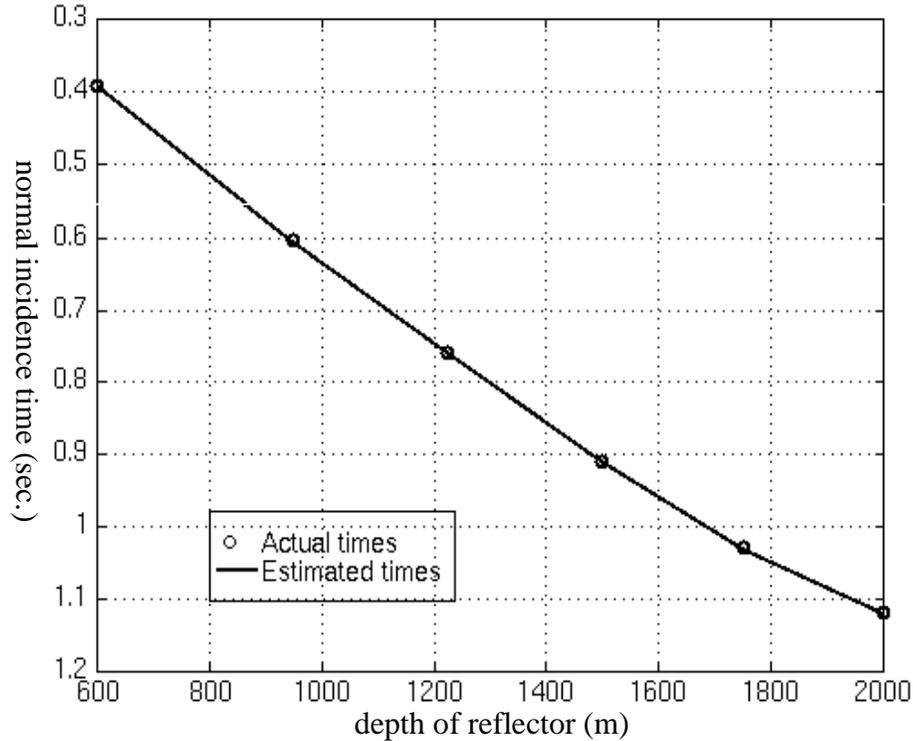Fig. 4.Traveltimes for the direct and reflected P-wave arrivals for borehole receiver at a depth 500m for the model.

Fig. 5.Normal incidence times estimated after semblance analysis match remarkably well with the actual times.

Moveout correction of converted-wave arrivals

Tessmer and Behle (1988) showed that a hyperbolic approximation to traveltimes can be used for converted-wave arrivals on the surface. Since in the VSP, asymmetry in the raypath is common to both pure P-wave and converted-wave arrivals, we simply extend the formulae for the pure P-wave arrivals (Equations A7 and A10) to the converted-wave arrivals in the VSP. Equations (A11) and (A12) then represent the traveltimes and *rms* velocity for converted-wave arrivals in the VSP.

The converted-wave arrivals need to be either corrected to normal incidence P-S times or approximated to normal incidence P-P times. To correct the converted-waves to normal incidence P-S times in a manner similar to the procedure outlined in Figure 2, one would need the downgoing direct S-wave arrival times. These may be available in the form of S-wave arrivals from P-S transmissions at layer interfaces.

These would give accurate estimates of zero-offset times for the downgoing S-wave only if these conversions occurred very near the surface. In Figure 8, however, we show a schematic diagram to correct the converted-wave arrivals to approximate normal incidence P-P times using the P-wave direct arrivals.

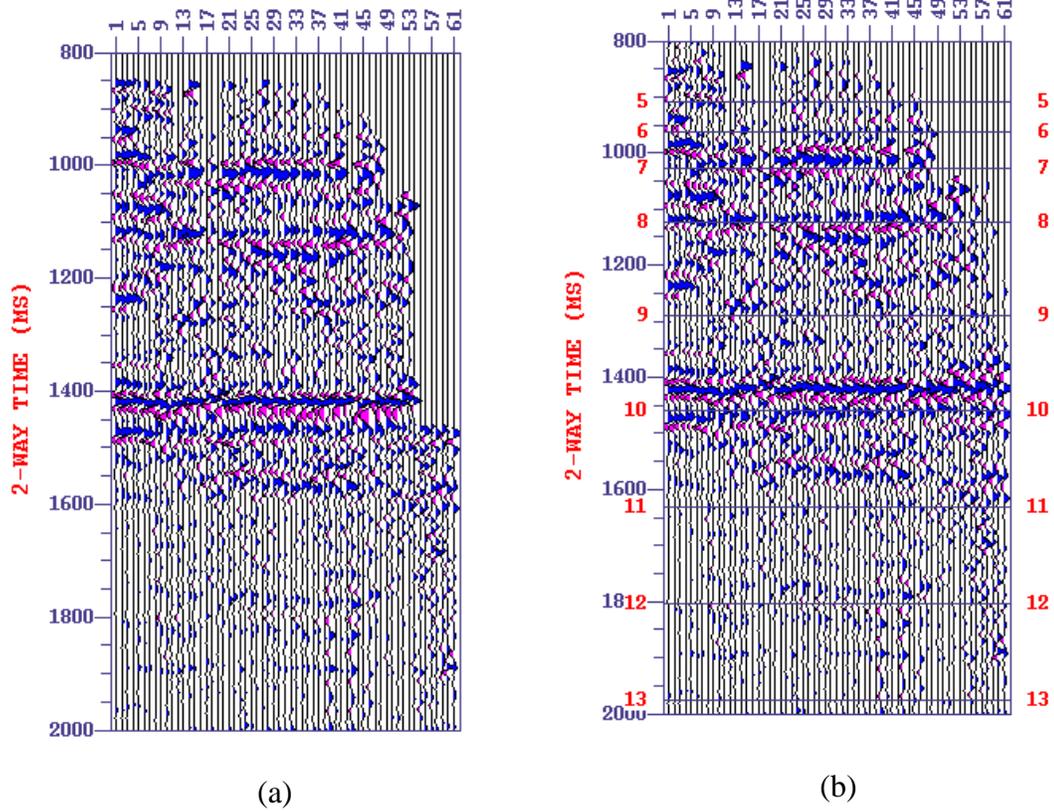(a)   (b)

Fig. 6.3-D VSP vertical component upgoing waves from receiver depth 400m corrected to normal incidence time (a) after semblance analysis and (b) using raytracing. Overlain on (b) are the numbers of the layer interfaces in the model used for raytracing.
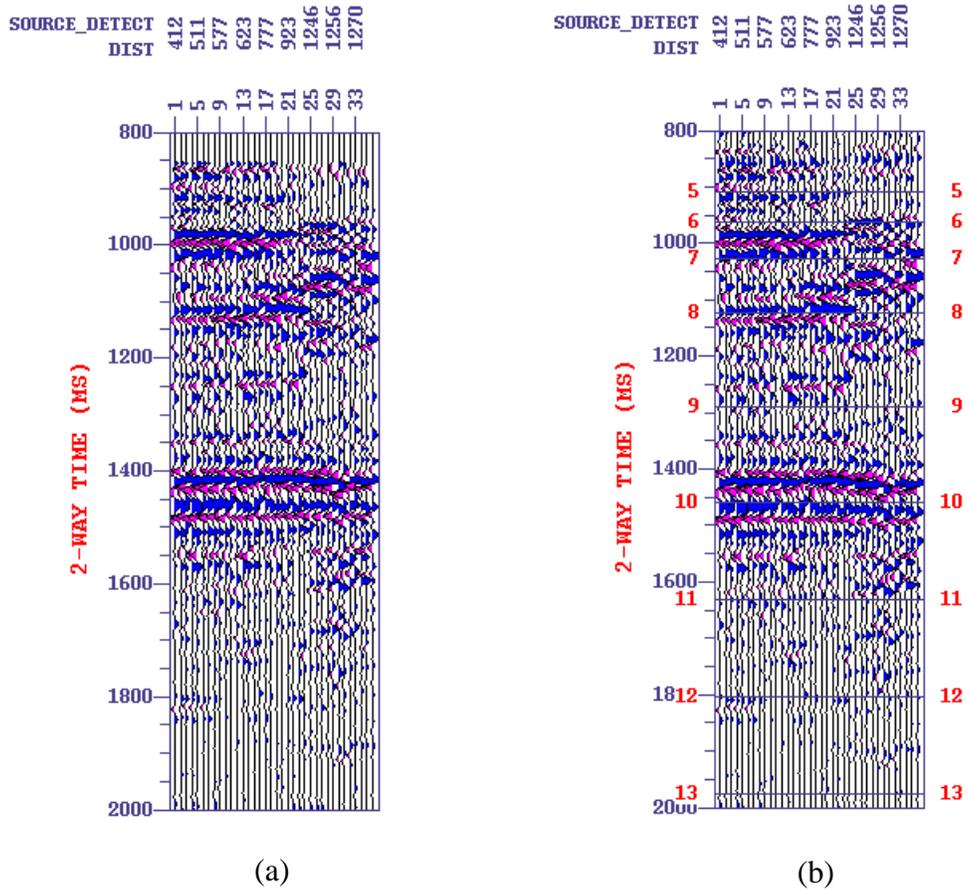
(a) (b)

Fig. 7.3D-VSP vertical component upgoing waves from receiver depth 910m corrected to normal incidence time (a) after semblance analysis and (b) using raytracing. Overlain on (b) are the numbers of the layer interfaces in the model used for raytracing.

SYNTHETIC

Synthetic converted-wave traveltimes were generated for the same model (Figure 3) using raytracing for the same source-receiver geometry. Following the steps outlined in Figure 8, the P-P normal incidence times (Figure 9) for each of the converted-wave reflections at borehole receiver depth of 500m were determined. We observe that the estimated P-P normal incidence times are reasonably accurate for all events.In fact, when V_P/V_S is close to 2 (see Figure 3), the estimated times are nearly the same as the actual times.

Dix interval velocities

A Dix formula (Appendix B) is used to estimate P-wave interval velocities of layers from the P-P stacking velocities. Estimates of interval velocities obtained during the moveout correction of the synthetic P-P traveltimes are compared with the actual model (Figure 10). The estimated velocity-depth model using the Dix formula is very similar to the actual model despite the assumption of stacking velocities being equal to the *rms* velocities. However, when events are closely spaced in time, the estimates deviate more from the actual values as observed in the case of the last two events.

Using the same procedure, the estimated model for the Blackfoot 3D-VSP data is compared with the one used in Zhang et. al. (1996). The two models differ each other to a large extent although the general trend is the same in both the models.

VSPCDP TRANSFORMATION

Conventionally, reflection points are mapped using raytracing in the VSPCDP transformation process. In simple geologies, approximate methods such as in Stewart (1991) could also be used in the VSPCDP transformation without much loss in accuracy. We use one such method and demonstrate that approximate methods can also provide reasonably accurate high-resolution 2D/3D-images in simple geologies.

VSPCDP mapping of pure P-wave reflections

The offset x_B of the reflection point from the well over a homogeneous single-layered earth is calculated in Stewart (1985) as

$$x_B = \frac{x}{2}[\frac{vt_v - 2z}{vt_v - z}]$$

(1)

where x, v, t_v, z are the source-receiver offset, constant velocity of the homogeneous single-layered medium, normal incidence time of reflection and depth of the receiver respectively.

We adapt Equation 1 which is valid for a single-layered medium to a multi-layered medium by simply substituting the stacking velocity $\bar{v}$ (assumed equal to *rms* velocity) in place of the constant velocity v and calculate the offset x_B of the reflection point from the well. Such an approximate approach to map the reflection points is simply a continuation of the VSP processing flow.
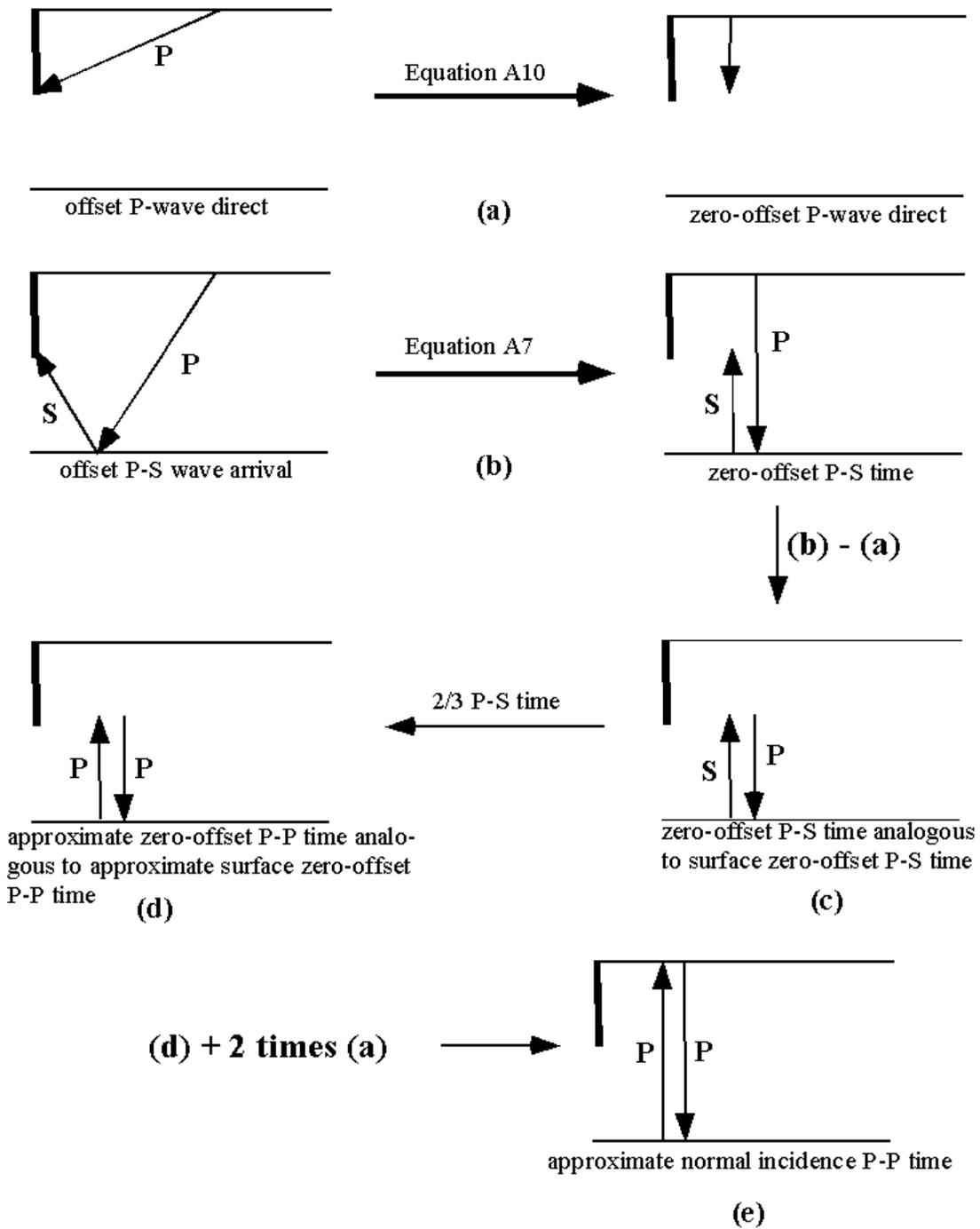
Fig. 8.(a) Correct the P-wave direct arrivals to a zero-offset time using Equation A10. (b)Correct the reflected converted-wave arrival times to zero-offset reflection time using Equation A11. (c)Subtract (a) from (b) to get zero-offset P-S times analogous to surface seismics. (d) Approximate normal incidence P-P time from receiver depth to the reflector. (e)Adding (d)+2*(a) gives the approximate P-P normal incidence time for the reflector.
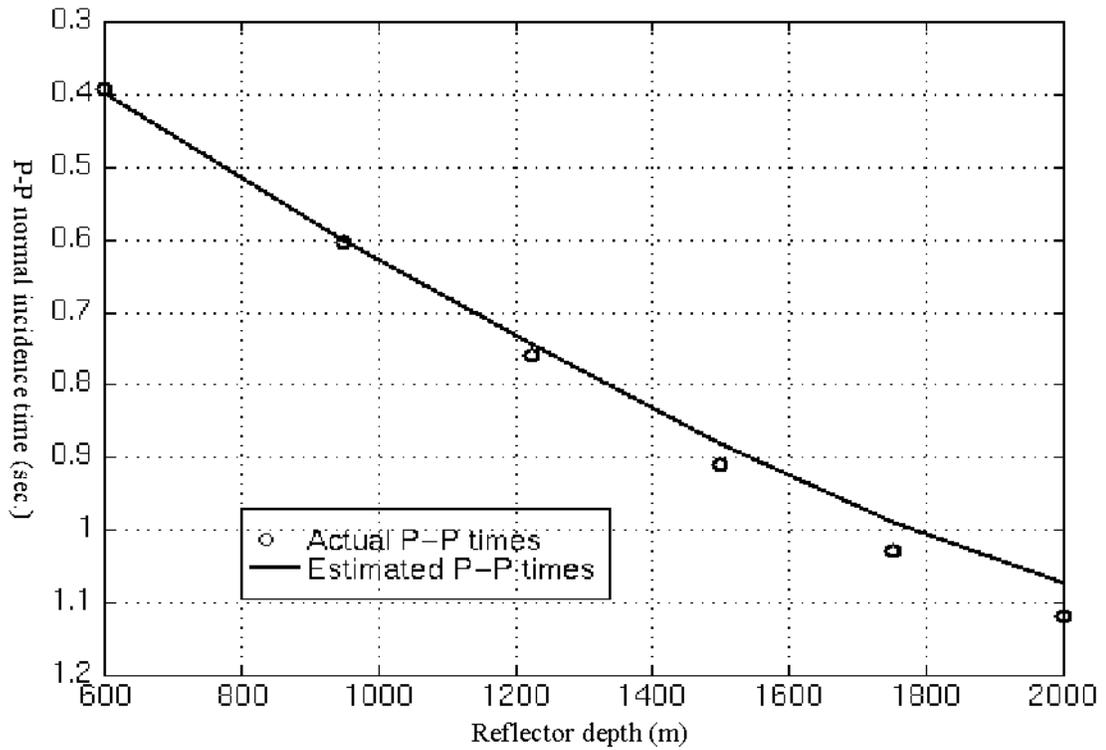
Fig. 9.P-P normal incidence times estimated after semblance analysis of converted-waves match reasonably well with the actual times especially where V_P/V_S is close to 2.

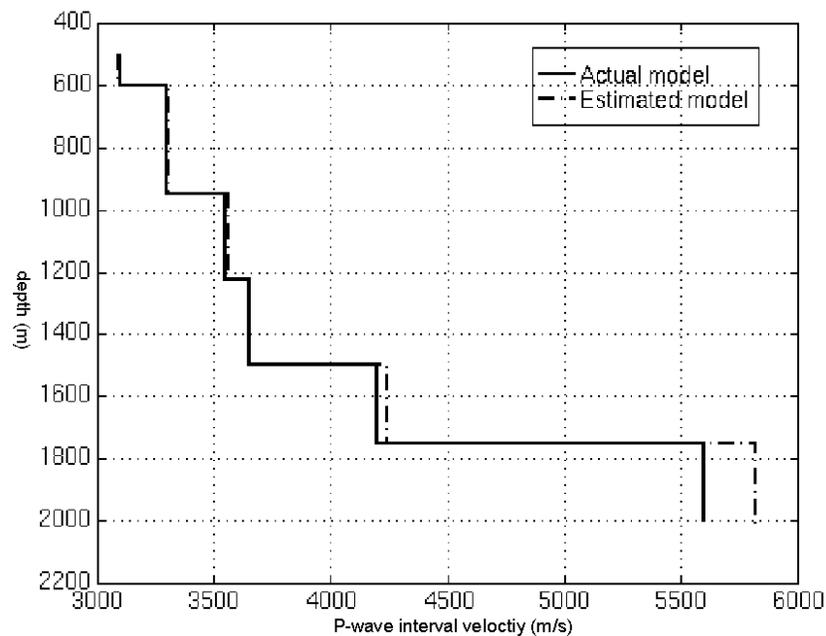

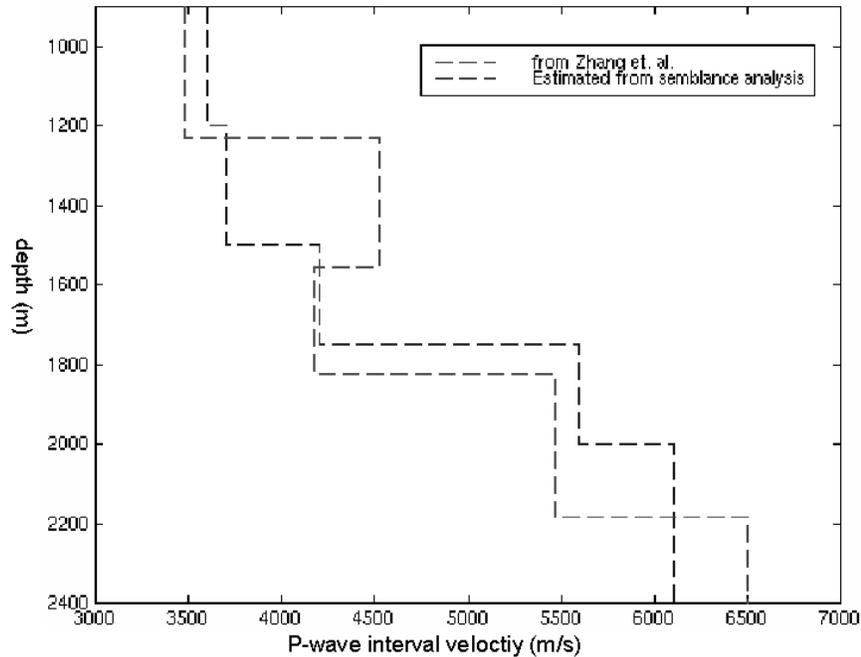Fig. 10.Dix estimates of the model compared with the actual model.

Fig. 11.Dix estimates of the model for the Blackfoot 3-D VSP compared with the model from Zhang et. al.(1996).

It only uses output from the normal moveout correction after amplitude semblance analysis and ,therefore, requires no model-building.

After the absolute offset x_B is calculated, (x, y) coordinates of the reflection point on the survey map are calculated (see Appendix C) and the reflection point mapped onto the survey map.

SYNTHETIC

The stacking velocities and normal incidence times for each of the pure P-wave reflections are obtained after the moveout correction of synthetic traveltimes (Figure 4) using amplitude semblance analysis. Then the reflection points were mapped using both 2-D raytracing mapping and the approximate mapping procedure outlined above.

From Figure 12, we observe that the approximate reflection points for the synthetic (Figure 4) at short-offsets are accurate when compared to those obtained from raytracing. Similarly, even at large offsets 2450m (Figure 13) the approximate mapping is accurate for practical purposes. The final image obtained by stacking reflections common to a bin cell will, therefore, be nearly the same using both the mapping methods. Figures 14 and 15 display the reflection point maps for all source-receiver offsets using both the methods to signals at receiver depths of 500m and 1000m respectively.

BLACKFOOT 3-D VSP

VSPCDP transformation of the vertical component Blackfoot data was also performed using both 2-D raytracing and the approximate mapping method. A 75m by 75m bin with an overlap of 10m was used in the VSPCDP transformation. Figures 16 and 17 are the VSPCDP transformed data from bins closer to the drilled well (see Zhang et. al., 1996 for survey details) in the south-north and east-west direction respectively. It is observed that the final image obtained using the approximate mapping method appears to have a higher fold compared to the raytracing method. One reason for this is that the approximate method maps the reflection points closer to the well than the actual reflection coordinates. Another reason could be that moveout correction using semblance analysis aligns events marginally better than raytracing moveout correction (Figures 6 and 7). Overall, it is observed that the final 3-D seismic image obtained using the two methods resemble each other to a large extent.

VSPCCP mapping of converted-wave reflections

Conversion points of converted-waves can be accurately established only by raytracing even for surface seismics. Conventionally, for VSP surveys, raytracing is used to determine the conversion points in the VSPCCP transformation. However, since in 3-D VSP surveys raytracing can be a time-consuming process, alternate methods are also desired. As seen in the earlier section, pure P-wave reflections could be mapped accurately for all practical purposes without using a raytracing routine. A similar procedure is also desired of converted-waves in the VSPCCP transformation process.

In surface surveys, the simplest method of CCP gathering is the asymptotic approximation to the conversion point (Fromm et. al., 1985; Chung and Corrigan, 1985). The asymptotic approximation gives the horizontal distance of the conversion point from the source point. In other words, it gives us an approximate offset of the conversion point from the reflection point of pure P-wave arrivals for the same source-receiver configuration. Similarly for VSP surveys, if we know the reflection point of pure P-wave arrivals, the corresponding conversion point for the converted-wave arrival with the same geometry could be determined by using the asymptotic approximation to the reflection point.

An essential step in the above approximate mapping procedure is determining the corresponding P-P normal incidence time and P-P *rms* velocity for a converted-wave event. The approximate P-P normal incidence time is determined from the previous sections (Figure 8) and the approximate P-P *rms* velocity using Equation D5 These are then used to compute the reflection point of the P-wave arrival using the approximate mapping procedure in the previous section. The conversion point of the converted wave is then determined using an asymptotic approximation to the calculated reflection point.
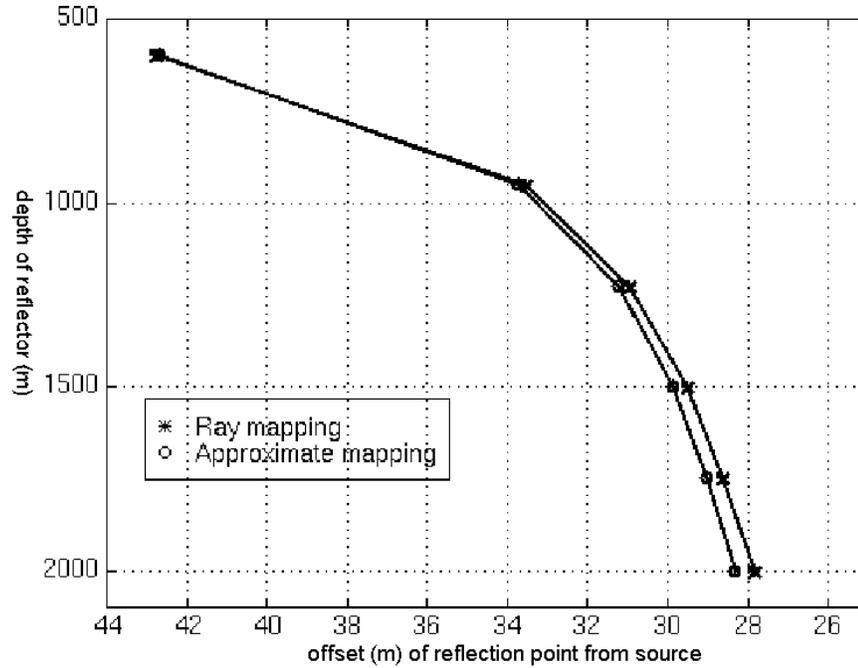
Fig. 12.Comparision of mapped reflection points for events in figure 4 using both raytracing and the approximate method for source at 50m offset from well with borehole receiver at 500m depth.
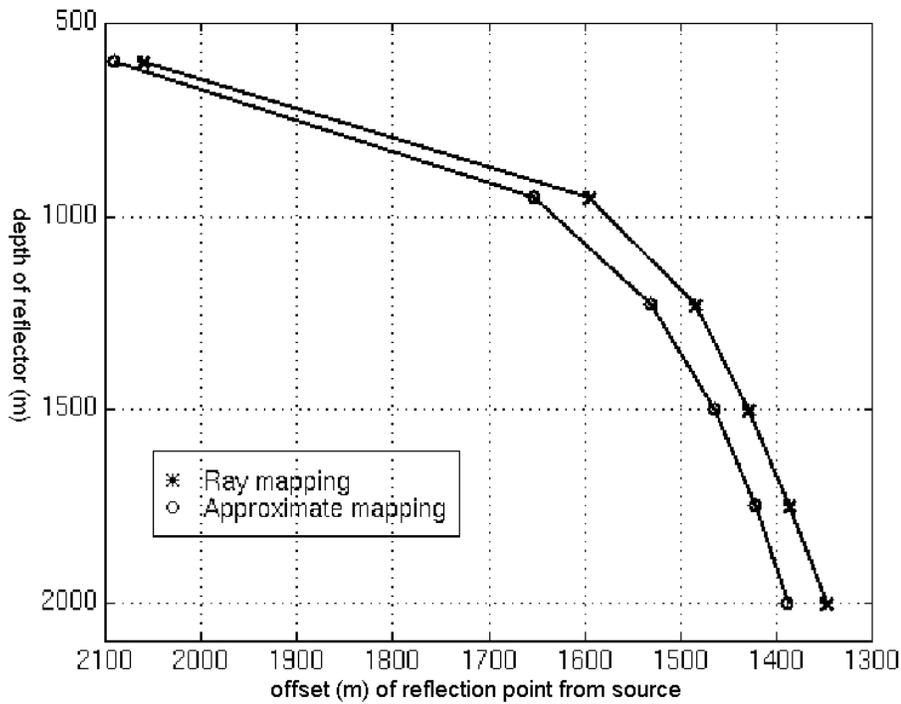

Fig. 13.Comparision of mapped reflection points for events in figure 4 using both raytracing and the approximate method for source at 2450m offset from well with borehole receiver at 500m depth.
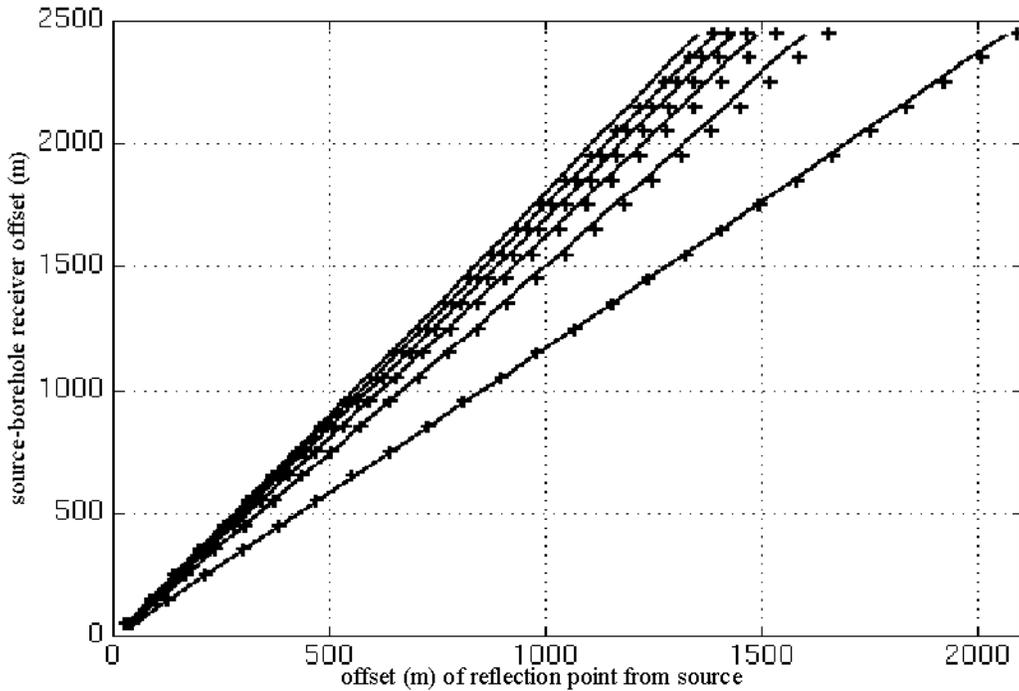
Fig. 14.Comparision of mapped reflection points for events in figure 4 using both raytracing and the approximate method for sources at 50-2450m offset from well with borehole receiver at 500m depth. The asterisks represent the approximate maps.
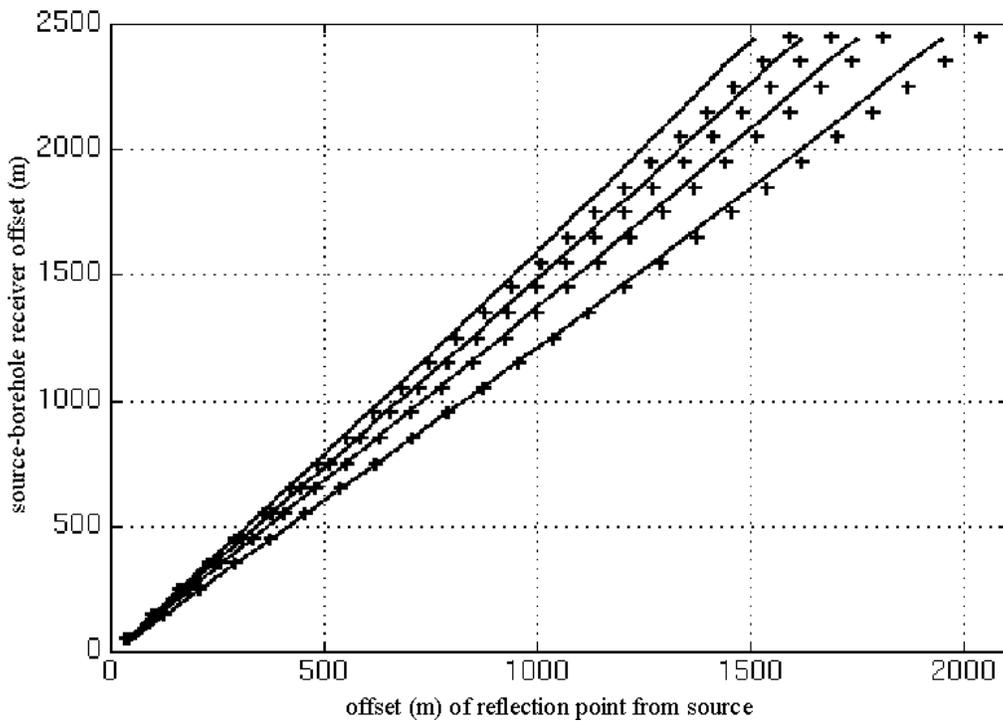

Fig. 15.Comparision of mapped reflection points for events using both raytracing and the approximate method for sources at 50-2450m offset from well with borehole receiver at 1000m depth. The asterisks represent the approximate maps.

Fig. 16.VSPCDP transformation of the vertical component Blackfoot 3D-VSP data (a)using the approximate mapping method and (b)using. 2D raytracing. Displayed are traces from bins close to the drilled well (shown in figure 9) in the south-north direction.
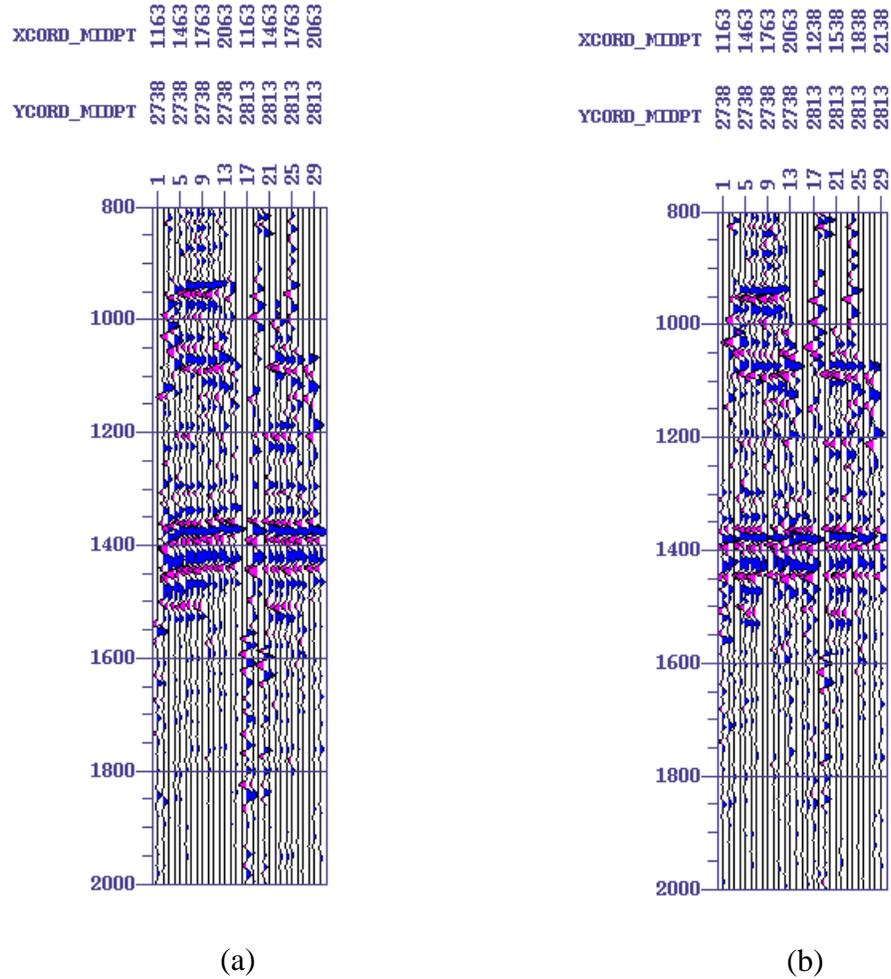
(a)   (b)

Fig. 17.3D-VSPCDP transformation of the Blackfoot 3D-VSP data (a)using raytracing and (b)using the approximate mapping method. Displayed are traces from bins close to the drilled well (shown in figure 9) in the east-west direction.

SYNTHETIC

Synthetic P-S arrivals for the model (Figure 3) were approximately mapped using the above procedure. Figure 18 shows a comparison of the estimated P-P *rms* velocities using Equation D5 with the actual P-P *rms* velocities for the reflectors. Here *rms* velocities refer to the stacking velocities in each case. The P-P *rms* velocities were estimated from the converted-wave arrivals by restricting the source-borehole receiver offsets to less than 500m. We observe that the estimated values are close to the actual values obtained from the P-P amplitude semblance analysis. A comparison of the approximately mapped conversion points with those mapped using raytracing show that the approximate mappings are comparable (Figures 19 and 20), except in the case of the reflector closest to the receiver. This event was mapped beyond the source-receiver offset which violates the assumption of a horizontally layered earth used throughout this paper. The mapping for this event could be corrected either by simple extrapolation or by some numerical method. At the time this paper was written, further investigations into the influence of the P-P stacking velocity estimates from converted-waves is required to better understand the process before any application to real data.
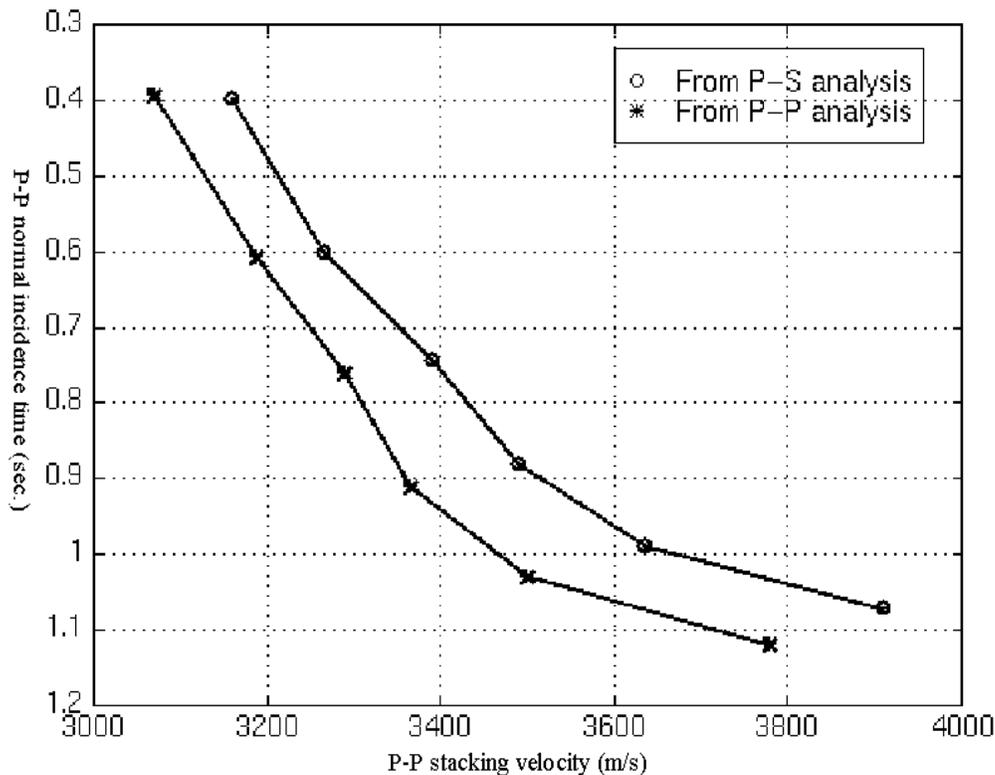

Fig .18.P-P stacking velocities obtained from amplitude semblance analysis of synthetic P-P and P-S arrivals.
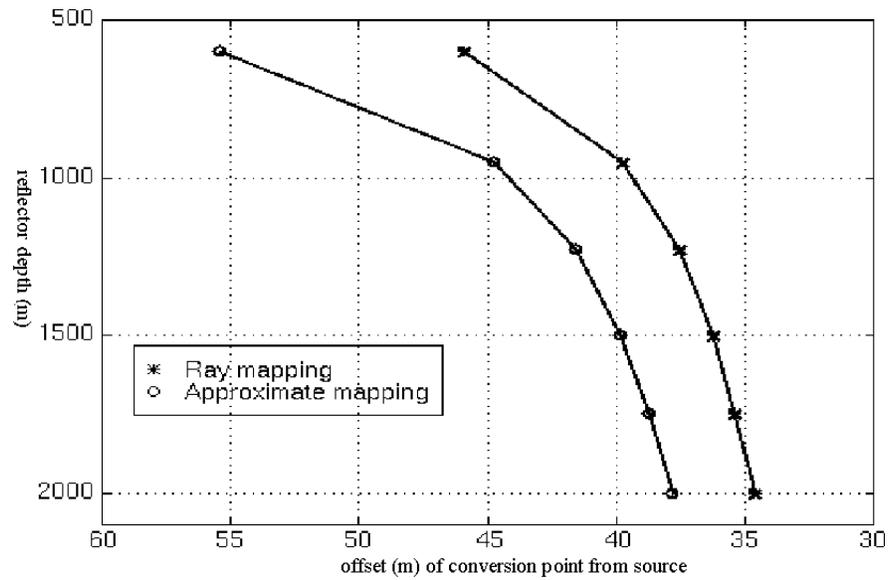
Fig. 19.Comparision of mapped conversion points for P-S synthetic using both raytracing and the approximate method. Source at 50m offset from well with borehole receiver at 500m depth.
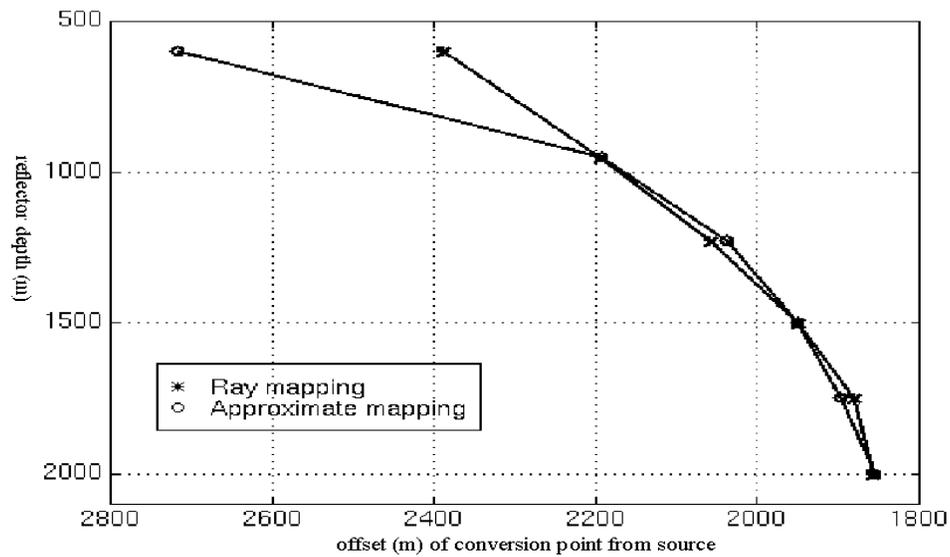

Fig. 20.Comparision of mapped conversion points for P-S synthetic using both raytracing and the approximate method. Source at 2450m offset from well with borehole receiver at 500m depth.

CONCLUSIONS

A two-term truncation of the power series expansion of the parametric *t-x* relationship for VSP recorded signals shows that the moveout of the arrivals is hyperbolic. This relation provides a statistical framework to correct VSP data in the receiver domain. The method based on amplitude semblance analysis is robust and accurately corrects VSP data to normal incidence time for a horizontally layered earth. Moveout correction using semblance analysis is easier to use compared to raytracing especially in the 3-D context where the data volume is large. 3-C VSP synthetics and vertical component of the Blackfoot 3C-3D VSP data corrected to normal incidence time after semblance analysis show remarkable correlation with that corrected using raytracing. VSPCDP transformation based on an approximate mapping method generated 3-D seismic image for the vertical component of the Blackfoot 3C-3D VSP data with reasonable accuracy when compared to the raytracing method. Preliminary tests on synthetic indicate the feasibility of extending the approximate mapping method to the VSPCCP mapping of converted-waves. The methods based on the assumption of a horizontally layered earth are an efficient way to obtain 2-D and 3-D seismic images in simple geologies. In complex geologies, however, these methods could precede more accurate imaging methods like migration to give a rough idea about the geology.

ACKNOWLEDGEMENTS

REFERENCES

Al-Chalabi, M., 1973, Series approximation in velocity and traveltime computations: Geophysical Prospecting, 21, 783-795.

Byun, B.S., Corrigan, D. and Gaiser, J.E., 1989, Anisotropic velocity analysis for lithology discrimination: Geophysics, 54, 1564-1574.

Chung, W.Y. and Corrigan, D., 1985, Gathering mode-converted shear waves: a model study, 55th Ann. Int. Mtg. Soc. Expl. Geophys., Expanded Abstracts, 602-604.

Dillon, P.B. and Thomson, R.C., 1984, Offset source VSP surveys and their image construction: Geophysical Prospecting, 32, 790-811.

Dix, C.H., 1955, Seismic velocities from surface measurements: Geophysics, 20, 68-86.

Fromm, G., Krey, Th. And Wiest, B., 1985, Static and dynamic corrections, in Ed. Dohr, G., *Seismic Shear Waves*, Handbook of Geophysical Exploration, Vol. 15a, Geophysical Press.

Hardage, B.A., 1983, Vertical Seismic Profiling, Part A-Principles:Geophys. Press.

Kohler, K. and Koenig, M., 1986, Reconstruction of reflecting structures from vertical seismic profiles with a moving source: Geophysics, 51, 1923-1938.

Moeckel, G.P., 1986, Moveout correction, bin and stack of offset VSP reflection data: 56th Ann. Int. Mtg. Soc. Expl. Geophys., Expanded Abstracts, 568-572.

Slotnick M.M., 1959, Lessons in seismic computing: Tulsa, SEG.

Stewart R.R., 1985, VSPCDP mapping: course notes *Borehole Seismic Methods: Acquiring, processing, and interpreting VSP surveys*, Western Atlas Logging Services, 1997.

Stewart R.R., 1991, Rapid map and inversion of P-SV waves: Geophysics, 56, 859-862.

Taner, T.M. and Koehler, F., 1969, Velocity spectra-Digital computer derivation and applications of velocity functions: Geophysics, 34, 859-881.

Tessmer, G. and Behle, A., 1988, Common reflection point data-stacking technique for converted waves: Geophysical Prospecting, 36, 671-688.

Wyatt, K.D. and Wyatt, S.B., 1984, Determining subsurface structure using the vertical seismic profile, in Eds. Toksoz, N.M. and Stewart, R.R., *Vertical Seismic Profiling, Part B-Advanced Concepts*, Geophys. Press.

Zhang, Q., Stewart R.R. and Sun, Z., 1995, 3-D VSP: Survey design and processing, CREWES Project Research report, V.7, Chpt. 34.

Zhang, Q., Stewart R.R., Parkin, J.M. and Sun, Z., 1996, Analysis of the Blackfoot 3C-3D VSP survey: CREWES Project Research Report, V.8, Chpt. 40.

APPENDIX A

Power series expansion for traveltimes of reflected signals in the VSP geometry

Taner and Koehler (1969) expanded the traveltime of reflected waves recorded on the surface over a horizontally layered medium into a power series as

$$t_n^2(x^2) = c_1 + c_2 x^2 + c_3 x^4 + c_4 x^6 + \ldots\ldots$$

(A1)

where the coefficients c_i (i=1,2,3,..) are functions only of the thickness and velocity of the layers.

Here we present an equivalent series expansion but for reflected waves recorded in the VSP geometry. The asymmetry of the downgoing and upgoing raypaths in the VSP geometry makes the derivation similar to that for converted waves as in Tessmer and Behle (1988). In a horizontally n-layered medium, the *t-x* relationship for reflected signals recorded in a borehole can be expressed in the parametric form (Slotnick, 1959)
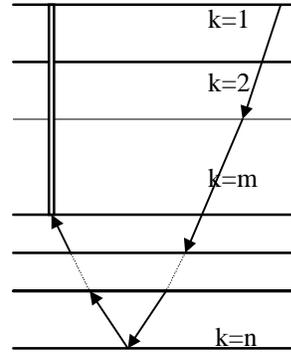
$$x = \sum_{k=1}^{k=n} \frac{p v_k d_k}{\sqrt{1 - p^2 v_k^2}} + \sum_{j=n}^{j=m} \frac{p v_j d_j}{\sqrt{1 - p^2 v_j^2}} \text{ , and}$$

$$t = \sum_{k=1}^{k=n} \frac{d_k / v_k}{\sqrt{1 - p^2 v_k^2}} + \sum_{j=n}^{j=m} \frac{d_j / v_j}{\sqrt{1 - p^2 v_j^2}}$$

where v_k and d_k are the P-wave velocity and thickness of the k-th layer and p is the ray parameter given by Snell's law as

$$p = \frac{\sin \theta_k}{v_k} \text{ , where } \theta_k \text{ is the angle of incidence of the ray at the k-th layer.}$$

Here for the sake of brevity, we assume that the receiver is located at the base of the (m-1)th layer, however, this assumption does not make a difference in the final results.

Using a Taylor series expansion of the function $(1 - p^2 v_k^2)^{-1/2}$, the above equations can be rewritten as

$$x = \sum_{k=1}^{k=n} p v_k d_k \sum_{i=1}^{\infty} \frac{1.3.5.....(2i-3)}{2.4.6.....(2i-2)} p^{2i-2} v_k^{2i-2} + \sum_{j=n}^{j=m} p v_j d_j \sum_{i=1}^{\infty} \frac{1.3.5....(2i-3)}{2.4.6.....(2i-2)} p^{2i-2} v_j^{2i-2}$$

$$= \sum_{i=1}^{\infty} \frac{1.3.5....(2i-3)}{2.4.6....(2i-2)} p^{2i-1} [\sum_{k=1}^{k=n} v_k^{2(i+1)-3} d_k + \sum_{j=n}^{j=m} v_j^{2(i+1)-3} d_j] \tag{A2}$$

Let $q_1 = 1$, $q_i = \dfrac{1.3.5....(2i-3)}{2.4.6....(2i-2)}$ and

$$a_i = \sum_{k=1}^{k=n} v_k^{2(i+1)-3} d_k + \sum_{j=n}^{j=m} v_j^{2(i+1)-3} d_j ;$$

Substituting the above in (A2) gives

$$x = \sum_{i=1}^{\infty} q_i a_{i+1} p^{2i-1}$$

Let $b_i = q_i a_{i+1}$, and, therefore,

$$x = \sum_{i=1}^{\infty} b_i p^{2i-1} \tag{A3}$$

Similarly, letting $\gamma_i = q_i a_i$, we get

$$t = \sum_{i=1}^{\infty} \gamma_i p^{2i-2} \tag{A4}$$

Substituting (A3) and (A4) in (A1) and comparing like powers of p^2 gives us the coefficients of the power series in (A1). Following Taner and Koehler (1969), the coefficients are calculated as follows:

$$c_1 = \gamma_1^2 = q_1 a_1^2 = a_1^2 = [\sum_{k=1}^{k=n} \frac{d_k}{v_k} + \sum_{j=n}^{j=m} \frac{d_j}{v_j}]^2 = t_{0r}^2 \tag{A5}$$

where t_{0r} is the zero-offset traveltime for the reflected P-wave arrival to the receiver in the borehole.

Similarly, $\quad c_2 = \dfrac{a_1}{a_2} = \dfrac{\displaystyle\sum_{k=1}^{k=n} d_k / v_k + \sum_{j=n}^{j=m} d_j / v_j}{\displaystyle\sum_{k=1}^{k=n} d_k v_k + \sum_{j=n}^{j=m} d_j v_j} = \dfrac{1}{(\bar{v})^2} \tag{A6}$

where $\bar{v}$ can be defined as the *root mean square (rms)* velocity for the reflected P-wave arrival with respect to the n-th reflector at the particular receiver depth.

Following the same procedure, we can derive other coefficients as well. However, a two-term truncation suffices for most practical purposes. Therefore, the traveltime-distance relationship for the reflected P-wave arrivals at a receiver in a borehole can be written as

$$t^2 = t_{0r}^2 + \frac{x^2}{(\overline{v})^2} \qquad\qquad (A7)$$

which is a hyperbola.

Following the same procedure for direct arrivals at the receiver, we get

$$c_1 = [\sum_{j=1}^{j=m-1} \frac{d_j}{v_j}]^2 = t_{0d}^2 \qquad\qquad (A8)$$

where t_{0d} is the zero-offset traveltime for the direct arrival to the receiver in the borehole.

Similarly, $$c_2 = \frac{\sum_{j=1}^{j=m-1} d_j/v_j}{\sum_{j=1}^{j=m-1} d_j v_j} = \frac{1}{(\overline{v})^2} \qquad\qquad (A9)$$

where $\overline{v}$ is the *rms* velocity for the direct arrival at the receiver.

Thus, a two-term truncation of the power series expansion for direct arrivals gives the hyperbolic *t-x* relationship

$$t^2 = t_{0d}^2 + \frac{x^2}{(\overline{v})^2} \qquad\qquad (A10)$$

Similarly, a hyperbolic approximation for the converted-wave traveltimes (following Tessmer and Behle, 1988) can be obtained,

$$t^2 = t_{0PS}^2 + \frac{x^2}{(\overline{v_{PS}})^2} \qquad\qquad (A11)$$

where t_{0PS} is the zero-offset traveltime to the borehole receiver for the converted-wave reflection. $\overline{v_{PS}}$ is the corresponding *rms* velocity given by

$$c_2 = \frac{a_1}{a_2} = \frac{\sum_{k=1}^{k=n} d_k/v_k + \sum_{j=n}^{j=m} d_j/\beta_j}{\sum_{k=1}^{k=n} d_k v_k + \sum_{j=n}^{j=m} d_j \beta_j} = \frac{1}{(\overline{v_{PS}})^2} \qquad\qquad (A12)$$

where β_j is the shear-wave velocity of the *j*-th layer.

The convergence properties of the traveltime expansions are the same as discussed in Al-Chalabi (1973).

APPENDIX B

Dix-type interval velocities

The Dix formula (1955) makes it possible to recover interval velocity for layers using the stacking velocities from the amplitude semblance analysis of surface data. Here, we show that the same formula can be used to determine P-wave interval velocities below the total depth of the well using the stacking velocities obtained from semblance analysis of VSP data.

For a reflected P-wave arrival from the n-th layer at a receiver just above the base of the m-th layer (see figure in main text), the *rms* velocity is given by

$$\overline{v}_n^{-2} = \frac{\sum_{i=1}^{n} d_i v_i + \sum_{j=n}^{m} d_j v_j}{\sum_{i=1}^{n} d_i / v_i + \sum_{j=n}^{m} d_j / v_j}$$

i.e.
$$\overline{v}_n^{-2} t_{rn} = \sum_{i=1}^{n} d_i v_i + \sum_{j=n}^{m} d_j v_j \tag{B1}$$

where t_{rn} is the zero-offset time for the reflected P-wave arrival to the receiver.

Similarly, for the n+1-th layer, we have

$$\overline{v}_n^{-2} t_{rn+1} = \sum_{i=1}^{n+1} d_i v_i + \sum_{j=n+1}^{m} d_j v_j \tag{B2}$$

Solving (C1) and (C2), the interval velocity v_n for the n-th layer is obtained as

$$v_n = \sqrt{\frac{\overline{v}_{n+1}^{-2} t_{rn+1} - \overline{v}_n^{-2} t_{rn}}{t_{rn+1} - t_{rn}}} \tag{B3}$$

which is the same form as that given in Dix (1955).

Similarly, for reflections from layer boundary just below the receiver, we use the zero-offset time and stacking (here used as *rms*) velocity of the direct arrivals to determine the interval velocity of the layer in which the receiver is located. Interval velocity of the layer in which the receiver is located can be calculated as

$$v_m = \sqrt{\frac{\overline{v}_m^2 t_m - \overline{v}_d^2 t_d}{t_m - t_d}}$$

(B4)

where v_m, v_d are the stacking (assumed as *rms*) velocities and t_m, t_d are the zero-offset times for reflections from the m-th layer and direct arrivals respectively.

Similarly, we can get the Dix formula for converted-waves as in Tessmer and Behle (1988).

APPENDIX C

Mapping the reflections points on the 3D survey geometry

Using simple coordinate geometry relations, the reflection coordinates are calculated as follows:

Let (x_1, y_1) and (x_2, y_2) be the source and receiver coordinates respectively. Then the reflection point (x, y) would lie on a line joining these two points given by

$$y = y_2 - m(x_2 - x)$$

(C1)

where $m = \dfrac{y_2 - y_1}{x_2 - x_1}$

Also, we have the relation

$$(y_2 - y)^2 + (x_2 - x)^2 = x_B^2$$

(C2)

Solving (C1) and (C2) for x, we get

$$x = x_2 \mp \frac{x_B}{\sqrt{m^2 + 1}}$$

(C3)

The sign is chosen such that the reflection point lies between the source and receiver locations. The value obtained from (C3) is then substituted in (C1) to give the (x, y) coordinates of the reflection point.

APPENDIX D

Approximate VSPCCP mapping

In this Appendix, we will first derive a formula to estimate the VSP P-wave stacking velocities from VSP converted-wave amplitude semblance analysis. We use these

values along with the approximately estimated normal incidence P-P times (Figure 8 in the main document) to calculate the approximate reflection point (Equation1 in the main document) of a pure P-wave arrival for the corresponding source-receiver geometry. The conversion point for the converted-waves is then an asymptotic approximation (Fromm et. al., 1985; Chung and Corrigan, 1985) to each of the calculated P-wave reflection point.

The *rms* velocity for converted-waves (V_{ps}) in a borehole receiver is given by

$$V_{ps}^2 = \frac{\sum_{i=1}^{i=n} \alpha_i^2 t_{\alpha i} + \sum_{j=n}^{j=m} \beta_j^2 t_{\beta j}}{t_{ps}} , \quad \text{where} \quad \alpha, \beta, t_\alpha, t_\beta, t_{ps}$$ denote the P-wave velocity, S-

wave velocity, P-wave traveltime, S-wave traveltime and total traveltime for the converted-wave respectively.
This can be rewritten as

$$V_{ps}^2 = \frac{\sum_{i=1}^{i=m-1} \alpha_i^2 t_{\alpha i} + \sum_{i=m}^{i=n} \alpha_i^2 t_{\alpha i} + \sum_{j=n}^{j=m} \beta_j^2 t_{\beta j}}{t_{ps}}$$

i.e.

$$V_{ps}^2 t_{ps} = \sum_{i=1}^{i=m-1} \alpha_i^2 t_{\alpha i} + \vartheta_{ps} \tag{D1}$$

where

$$\vartheta_{ps} = \sum_{i=m}^{i=n} \alpha_i^2 t_\alpha + \sum_{j=n}^{j=m} \beta_j^2 t_{\beta j} . \tag{D2}$$

From Equation (D1), we have

$$\vartheta_{ps} = V_{ps}^2 t_{ps} - \sum_{i=1}^{i=m-1} \alpha_i^2 t_{\alpha i} , \quad \text{which can be modified to}$$

$$\vartheta_{ps} = t_{0d} \left(\frac{V_{ps}^2 t_{ps}}{t_{0d}} - V_d^2 \right) \tag{D3}$$

where t_{0d}, V_d are the zero-offset time and *rms* velocity of the P-wave direct arrival. The quantity ϑ_{ps} is thus determined from the known quantities on the right-hand side of the equation.

Let $\vartheta_{pp} = \sum_{i=m}^{i=n} \alpha_i^2 t_\alpha + \sum_{j=n}^{j=m} \alpha_j^2 t_{\alpha j}$ and assuming $\alpha/\beta = 2$, we get

$$\vartheta_{pp} = 4\vartheta_{ps}/3$$

(D4)

The VSP P-wave reflection *rms* velocity (Equation A6) is, therefore, given by

$$V_{pp}^2 = \frac{\sum_{i=1}^{i=m-1} \alpha_i^2 t_\alpha + \vartheta_{pp}}{t_{pp}}, \quad \text{where} \quad t_{pp} \quad \text{is the zero-offset arrival time for the P-wave}$$

reflection to the receiver in the borehole.

The above expression is the same as

$$V_{pp} = \frac{V_d^2 t_{0d} + \vartheta_{pp}}{t_{pp}}$$

(D5)

Equation (D5) thus gives us an estimate of the VSP P-wave *rms* velocity from the amplitude semblance analysis of converted-waves (Figure 8).

The estimated VSP P-wave velocity and the P-P normal incidence time are then used to compute the approximate reflection point for the P-wave arrival to the borehole using Equation 1 (main document). The approximate P-wave reflection offset from the source x_{pp} is then used to determine the conversion point of the converted-wave for the same source-receiver geometry. Assuming $\alpha/\beta = 2$, the conversion point from the source is then given by $x_{ps} = \frac{4x_{pp}}{3}$.